Flux corrected finite-volume scheme for preserving scalar boundedness in large-eddy simulations

By M. Herrmann, G. Blanquart, and V. Raman

1. Motivation and objectives

Large-Eddy Simulation (LES) has emerged as the next generation simulation tool for handling industrially relevant turbulent reacting flows. Of particular interest is the use of LES for modeling complex combustors used both in power-production and aircraft engines (Ham *et al.* 2003; di Mare *et al.* 2004). Similarly, the chemical processing industry deals with a variety of turbulent flows that involve interaction of mixing and reaction with the final aim of controlling product selectivity and optimizing yield. As LES technique moves from being an academic tool to a practical simulation strategy, robustness of the LES solvers is a key issue to be answered. In low-mach number combustion, the staggered representation of the primary variables combined with an energy conserving scheme for the momentum equations has been shown to be a stable methodology for a wide variety of flows (Morinishi *et al.* 1998). In spite of the vast advancement in solving the momentum equations, the scalar transport equations that represent the species distribution inside the geometry and is thus key to predicting combustor performance, have not been studied in detail.

Numerical schemes for scalar transport equations are challenging from the viewpoint of stability. The advection equation solved using central difference based schemes can lead to oscillations and instabilities (Pierce 2001). To counter this problem, all known explicit schemes use an upwind bias that reduces numerical oscillations. As can be expected, this upwind bias reduces the numerical accuracy of the scheme and leads to artificial diffusion. In spite of this drawback, such schemes are widely used to their robust numerical stability. Many of these schemes suffer from one another drawback in that the species values are not bounded. In principle, a scalar transport equation solved using bounded initial and boundary conditions should preserve the boundedness (Pope 2000). In the present study, we consider the simulation of a conserved scalar, namely mixture fraction. Common combustion models use mixture-fraction to parameterize all species composition and is thus relevant to reactive flows. By definition, the solution to the mixture-fraction transport equation should always be in the set $[0, 1]$. The source of error in low-mach number formulations come from the staggering of the velocity and scalar variable locations. Usually, the velocity is defined at the cell-faces while the scalar is defined at the cell center. To compute the face based fluxes, an interpolative scheme is used based on a fixed stencil to obtain scalar values at the cell faces. Such interpolations do not impose a constraint on the scalar bounds which lead to oscillations around the local maximum and minimum values of the scalar.

Recently, a new class of schemes called Weighted Essentially Non-Oscillatory (WENO) schemes have been introduced that devise a total variation bounded (TVB) non-oscillatory scheme for advection type equations (Jiang & Peng 2000). Though these methods can be

extended to higher-order accuracy, the interpolative coefficients need to be reconstructed at each iterative loop. Again, extensions to complex unstructured grids are not straightforward and could be computationally expensive. In this work, a well-tested numerical scheme for scalars, namely the Quadratic-Upwind biased Interpolative Convective scheme (QUICK) (Leonard 1979) will be used. By switching between two interpolative functions, it will be shown that scalar boundedness as well as reduced oscillatory nature can be ensured. In addition, through detailed analysis of the numerical errors, it will be illustrated that the numerical accuracy is equivalent to the QUICK scheme.

2. Bounded QUICK scheme

It is known that a first-order upwind based interpolation is unconditionally bounded (within CFL restrictions) but can lead to large dissipative errors. In this work, we utilize the boundedness property of the first-order upwind scheme to formulate a dual valued stencil for the scalar. Each time-step is split into two sub-steps that can be constructed as a predictor-corrector algorithm. The predictor step moves the solution from the previous time-step to a predicted step. Locally, in cells where the predicted scalar solution is outside physical or acceptable boundaries, the interpolative scheme is switched to the full first-order upwind scheme while the rest of the domain uses the original QUICK stencil. Using this new stencil and the initial scalar field before the predictor step, the corrector step advances the scalar field to the next time level. This modified method is termed Bounded QUICK (BQUICK) scheme. In spite of the added local dissipation it is observed that the overall accuracy is not degraded and that the the boundedness is ensured to within velocity field divergence errors.

3. Numerical implementation

For clarity, the discussion in the following is limited to the one-dimensional case. Extension to two and three dimensions is straightforward.

The underlying numerical scheme of BQUICK is the original QUICK method (Leonard 1979) which has been implemented in both uniform and stretched grids. The advection time-stepping consists of two sub-steps termed predictor and corrector steps. In the predictor step the solution is advanced to the next time step using,

$$\phi^0(t) \overset{\text{QUICK}}{\longrightarrow} \phi^p(t+\Delta t)\,, \tag{3.1}$$

using cell face values $\phi^0_{i-1/2}$ calculated with the original QUICK scheme. Then, in the corrector step, all cells whose predicted values ϕ^p are outside their acceptable bounds $\phi_{\min}$ and $\phi_{\max}$ are discarded and recalculated using a first order approximation for the cell face values $\phi^1_{i-1/2}$ and $\phi^1_{i+1/2}$. All other cell faces retain their values from the predictor step. Figure 1 summarizes the algorithm of the BQUICK corrector step.

In practical LES computations, several sub-iterations are carried out in each time-step iteration to ensure numerical stability. In such cases, the above predictor-corrector step is executed in each sub-iteration with the initial scalar values determined by the field at the previous sub-iteration. The next section describes numerical tests to illustrate the performance and accuracy of the new scheme.

```
for all control volumes V_i do
  φ^1_{i-1/2} = φ^0_{i-1/2}
end for
for all control volumes V_i do
  if φ^p_i > φ_max or φ^p_i < φ_min then {revert cell update to first order}
    if u_{i-1/2} ≥ 0 then
      φ^1_{i-1/2} = φ^0_{i-1}
    else
      φ^1_{i-1/2} = φ^0_i
    end if
    if u_{i+1/2} ≥ 0 then
      φ^1_{i+1/2} = φ^0_i
    else
      φ^1_{i+1/2} = φ^0_{i+1}
    end if
  end if
end for
```

FIGURE 1. BQUICK corrector step.

4. Numerical tests

A series of tests are used to compare the new scheme with the original QUICK scheme and, in order to make a comparison with TVB based schemes, a 3rd order WENO scheme.

4.1. *1D tests*

To determine the order of accuracy, a sine wave function extending over a domain of $[0, 2\pi]$ is convected using a constant velocity and imposing periodic boundary conditions. Since the sine wave is a smooth function, numerical dispersion errors are minimized. Two different functions are used to test the effect of sharper curves. The first test uses as initial condition

$$Z(x) = \frac{1}{2}\left(\sin(\pi x) + 1\right). \tag{4.1}$$

The simulations are carried out on increasing resolution up to a grid of 1024 points. Using the exact solution, L_1, L_2 and L_∞ errors in the predictions are computed. Table 1 shows the errors in each simulation for the three different numerical schemes. It is seen from the L_2 error that the BQUICK and QUICK scheme both show slightly more than second order accuracy while the WENO scheme shows more than 4th order accuracy. The second function uses a sharper profile for the initial conditions.

$$Z(x) = \sin^4(\pi x). \tag{4.2}$$

Table 2 shows the errors as well as the accuracy estimates for the different numerical schemes. The QUICK and BQUICK scheme have retained second order accuracy for this profile. In fact, the BQUICK scheme shows almost identical results as for the previous test case. However, the WENO scheme shows a dramatic reduction in accuracy. The order of the scheme has dropped from over 4 in the previous case to between 2.5-3.5. As explained in the previous section, the WENO scheme uses an arbitrary smoothness factor that determines the extent of influence of the upwind biased correction. The weighting factor is determined by the gradients at the location which increases the lower order flux correction leading to reduction of the overall accuracy of the scheme.

Though the above test reveals the truncation error, scalar profiles in turbulent flow are rarely smooth and involve strong gradients. To test such a scenario a canonical 1-D

TABLE 1. Accuracy for $Z(x) = \frac{1}{2}(\sin(\pi x) + 1)$

Method	N	L_∞ error	L_∞ order	L_1 error	L_1 order	L_2 error	L_2 order
Quick	128	1.07E-04		6.81E-05		6.69E-06	
	256	2.56E-05	2.06	1.63E-05	2.06	1.13E-06	2.56
	512	6.33E-06	2.02	4.03E-06	2.02	1.98E-07	2.52
	1024	1.58E-06	2.00	1.00E-06	2.00	3.49E-08	2.50
Bquick	128	1.15E-04		7.27E-05		6.97E-06	
	256	2.85E-05	2.01	1.75E-05	2.06	1.18E-06	2.57
	512	7.24E-06	1.98	4.27E-06	2.03	2.04E-07	2.53
	1024	1.92E-06	1.92	1.05E-06	2.03	3.56E-08	2.52
WENO-3	128	7.00E-03		1.40E-03		2.10E-04	
	256	1.28E-03	2.45	1.61E-04	3.12	2.01E-05	3.39
	512	8.94E-05	3.84	1.16E-05	3.80	8.84E-07	4.51
	1024	3.11E-06	4.85	1.27E-06	3.19	4.45E-08	4.31

TABLE 2. Accuracy for $Z(x) = \sin^4(\pi x)$

Method	N	L_∞ error	L_∞ order	L_1 error	L_1 order	L_2 error	L_2 order
Quick	128	3.55E-03		1.81E-03		1.83E-04	
	256	6.54E-04	2.44	3.29E-04	2.46	2.38E-05	2.95
	512	1.45E-04	2.18	7.20E-05	2.19	3.71E-06	2.68
	1024	3.49E-05	2.05	1.73E-05	2.06	6.32E-07	2.55
BQuick	128	3.59E-03		1.77E-03		1.86E-04	
	256	6.51E-04	2.47	3.27E-04	2.43	2.42E-05	2.94
	512	1.45E-04	2.17	7.22E-05	2.18	3.74E-06	2.70
	1024	3.49E-05	2.05	1.74E-05	2.05	6.34E-07	2.56
WENO-3	128	6.70E-02		1.49E-02		2.02E-03	
	256	2.41E-02	1.48	3.27E-03	2.19	4.06E-04	2.32
	512	6.35E-03	1.92	5.15E-04	2.67	5.73E-05	2.83
	1024	9.03E-04	2.81	5.35E-05	3.27	4.26E-06	3.75

convection Jiang & Shu (1996) problem is used. As initial conditions, a profile consisting of several shapes with sharp gradients are distributed across the domain. A uniform velocity field is imposed with periodic boundaries. A fourth-order Runge-Kutta based time-integration is used to minimize temporal errors. The simulation is carried out for

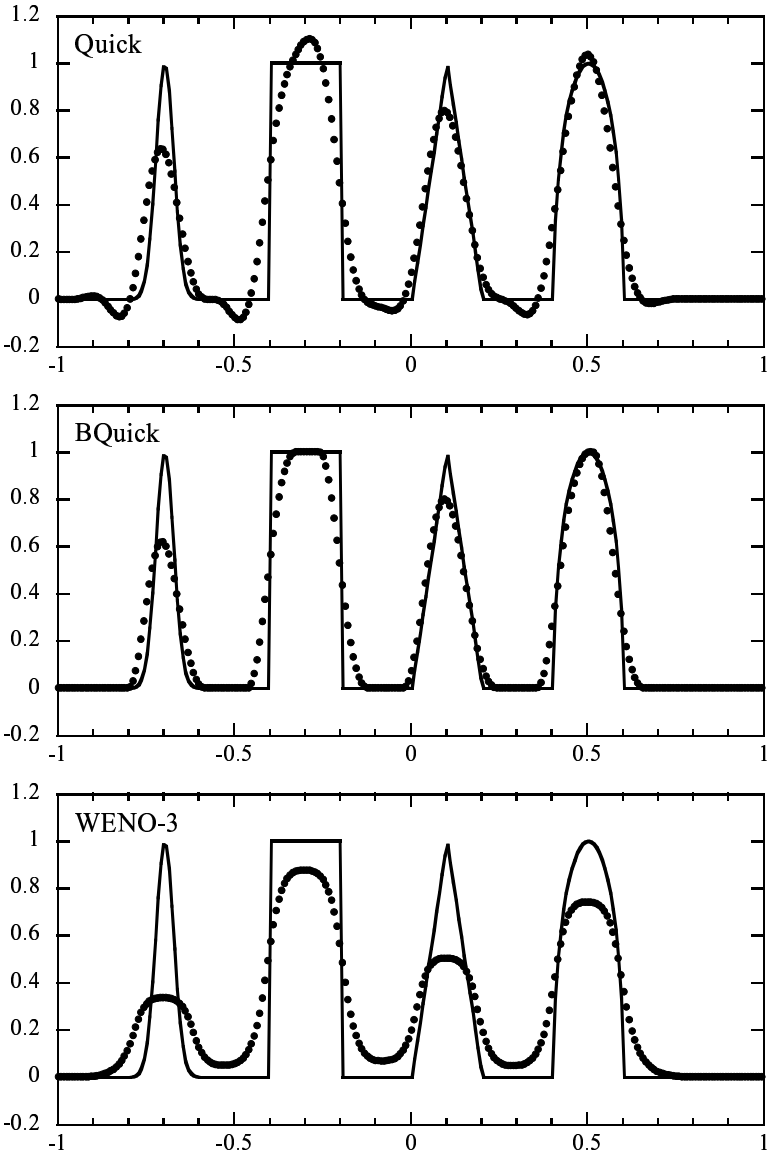

FIGURE 2. 1-D convection test case. Comparison of numerical schemes after 4 rotations. Lines indicate exact result while symbols denote numerical computation.

4 rotations where each rotation is defined as the time taken for the initial profile to be convected back to its initial location. Figure 2 compares the results from the QUICK, BQUICK and WENO schemes. It can be seen that the QUICK scheme locally exceeds the initial bounds of the scalar. In addition, it exhibits oscillations near regions of sharp gradients. The BQUICK scheme on the other hand maintains the boundedness accurately while also reducing the unphysical oscillations. Interestingly, the BQUICK scheme performs better at capturing the peaks as compared to the WENO scheme. This clearly illustrates the negative effects of TVB type damping of scalar fluctuations that are crucial in LES simulations.

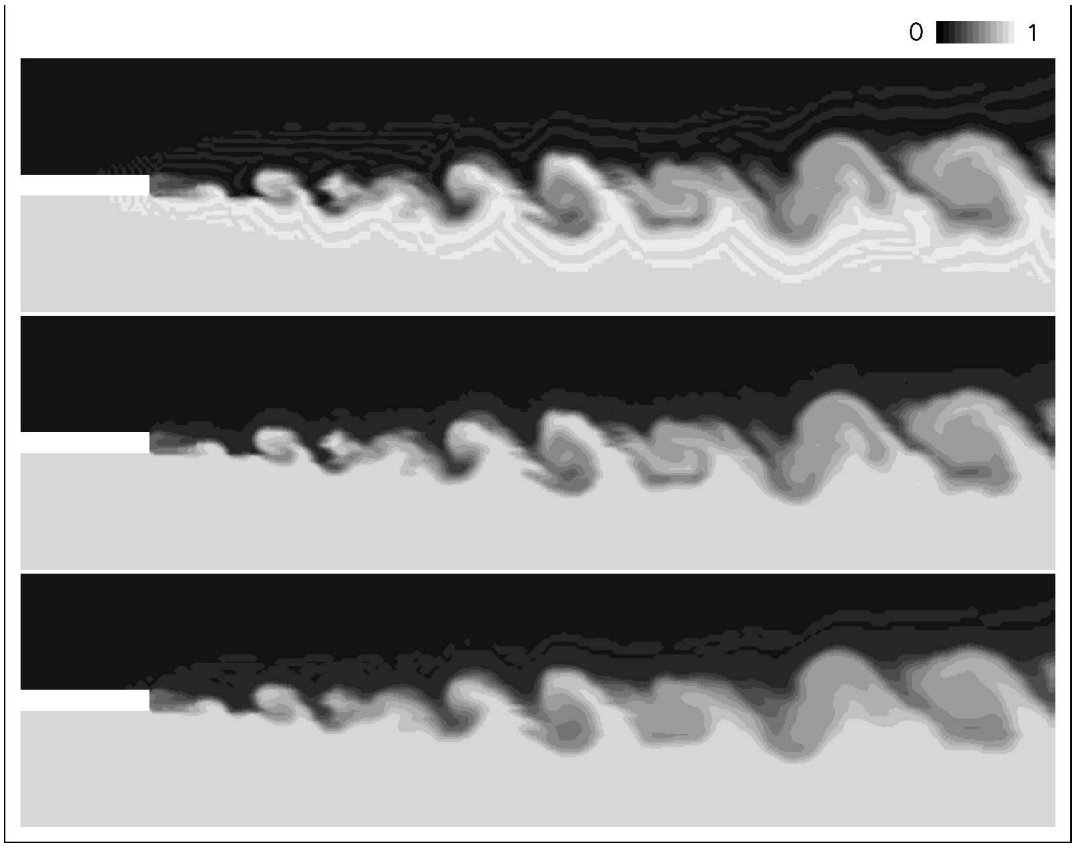

FIGURE 3. Two-dimensional profile of the instantaneous mixture-fraction in a mixing-layer. The top figure shows the QUICK results clipped between 0 and 1. The middle figure shows the BQUICK results. The bottom figure shows the WENO results.

4.2. *Mixing layer tests*

The second set of tests consists of an actual multi-dimensional implementation of the three schemes (QUICK, BQUICK and WENO). Two configurations are investigated: a spatially evolving mixing layer using LES and a temporal mixing layer using DNS. The equations for both of these simulations are solved in non-dimensional units using a domain decomposition based parallel solver. Further details of the code as well as the sub-filter models used (in the case of LES) can be found in Pierce (2001).

4.2.1. *Spatial mixing layer*

The inflow bulk velocities of the two streams are set to a ratio of 1:2.5 with laminar profiles. A splitter plate initially divides the streams and the mixing layer starts at X=0. The domain, including the splitter plate stretches for 80 units while the width is set at 20 units. Figure 3 shows the instantaneous scalar concentration using the three schemes. The QUICK scalar field has been clipped between 0 and 1 while the BQUICK and the WENO scalar field maintain the bounds. Visually the differences between the QUICK and BQUICK schemes are not noticeable. On the other hand the WENO scalar field is smoother than the two other schemes. To better understand the effect of the BQUICK scheme, crosswise scalar profiles are plotted (Fig. 4). It is seen that the BQUICK main-

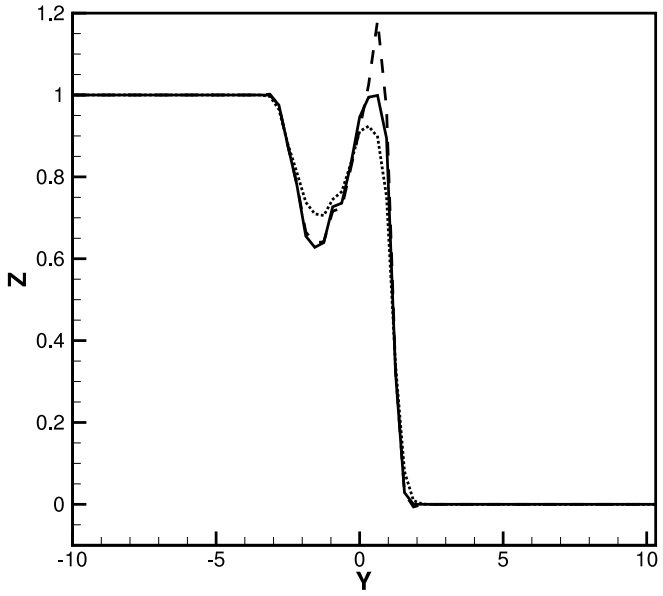

FIGURE 4. Cross-stream profile of mixture fraction obtained in the mixing layer at an arbitrary downstream location. Dashed lines show the QUICK profile, solid lines show the BQUICK profile and, dotted lines show the WENO profile.

tains the same profile as the QUICK scheme away from the bounds of the scalar while closer to 0 and 1, the BQUICK adjusts itself to maintain the bounds. The WENO profile is also bounded but it is much smoother than the BQUICK profile and does not show the same scalar gradient. The lower-order correction for the BQUICK at the bounds in composition space has limited impact on the physical transport. To further substantiate this argument, time-averaged profiles of both the scalar as well as the scalar RMS value are plotted in Fig. 5. Increased numerical diffusion will reduce the RMS fluctuations. However, the profiles indicate that the BQUICK correction has no substantial effect on the accuracy of the scheme. The upwind correction does not lead to substantial numerical diffusion that is characteristic of the first-order upwind scheme. As such, the corrections are applied in a very small fraction of the computational domain and hence the RMS fluctuations are not damped by dispersion errors. On the other hand the time-averaged WENO profile of scalar RMS shows much more dissipation than the BQUICK scheme: the RMS fluctuations of the scalar are damped by about 20% compared to the QUICK/BQUICK RMS fluctuations.

4.2.2. *Temporal mixing layer*

The computational domain used for the simulation of the temporal mixing layer was initially divided into two streams separated by an interface located at $Y = 0$. The initial mean velocity distribution is given by a hyperbolic tangent velocity profile. Three dimensional perturbations with wavelength of up to a quarter of the domain length were superimposed on the mean velocity profile. The different variables were non-dimensionalized

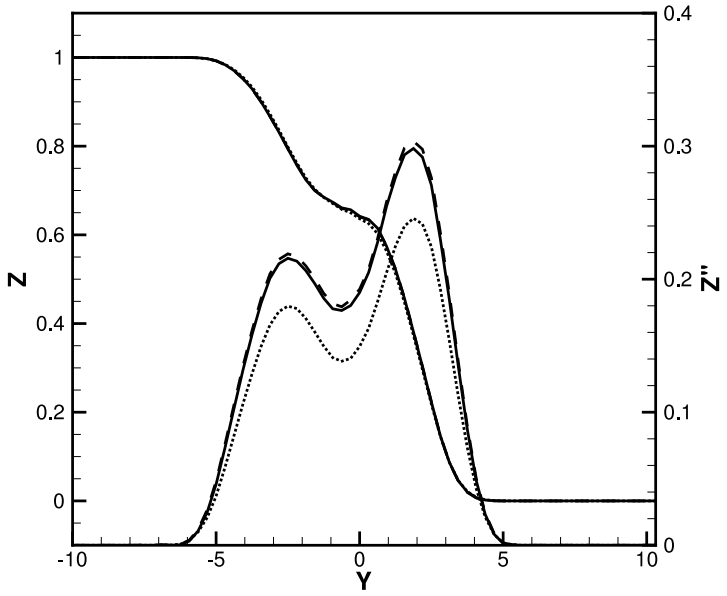

FIGURE 5. Time-averaged cross-stream profile of mixture-fraction obtained in the mixing layer at an arbitrary downstream location. Dashed lines show QUICK profiles, solid lines show BQUICK profiles and, dotted lines show WENO profiles.

using the initial vorticity thickness (δ_ω) and the mean velocity difference between the two streams. Based on these definitions, the initial Reynolds number was $Re_{\omega,0} = 435$. The simulation was performed on a grid with $256 \times 256 \times 256$ control volumes. Figure 6 shows the one-dimensional streamwise energy spectrum of the streamwise velocity component at $t = 92$. For reference, the slope of the inertial range is indicated. The energy spectrum is in good agreement with previous work (Vreman 1995).

To better isolate the effect of numerical dissipation by the different schemes, the scalar transport equation was solved without molecular diffusion. In such a configuration the energy cascade still occurs but the energy should not be dissipated at the lowest length scales. However numerical dissipation introduced by the schemes will prevent the energy from piling up at the smallest length scales. Figure 7 shows the one-dimensional energy spectra of the scalars. The inertial range is accurately captured by the three schemes. However numerical dissipation damps out the energy at the highest wave numbers. As is can be observed, the WENO scheme introduces more numerical dissipation than the QUICK and BQUICK schemes. This result can be further ascertained by considering the RMS fluctuations of the scalar (Fig. 8). The upwind correction of the BQUICK scheme has little effect on the RMS fluctuations. Once again the fraction of computational domain where the correction is applied is very small. On the other hand the WENO profile shows lower RMS value (of about 15%) compared to QUICK/BQUICK profiles. The additional numerical dissipation introduced by the the WENO scheme also affects the shape of the material interface. The WENO scheme does not only dissipate more than the BQUICK scheme it also reduces the total surface area of the interface. Figure 9 show the iso-surface

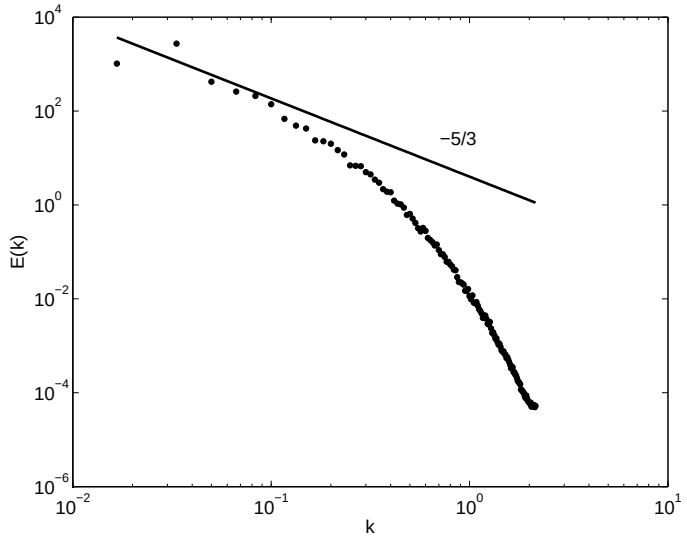

FIGURE 6. One-dimensional (planar averaged) streamwise energy spectrum of the streamwise velocity component at $Y = 0$ ($t = 92$).

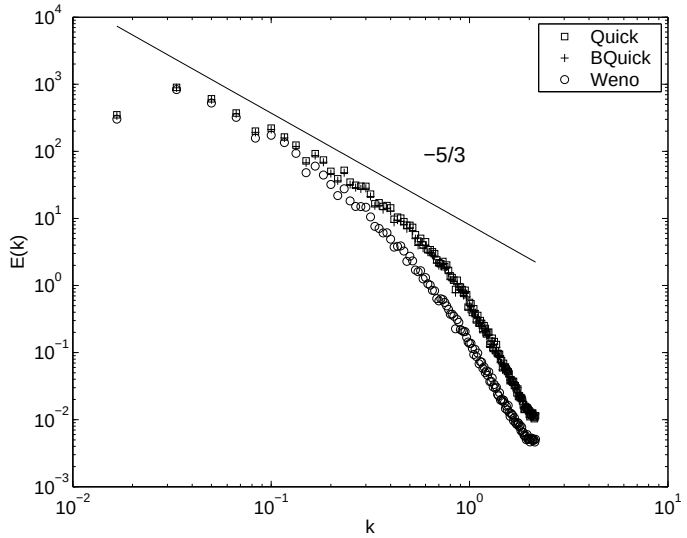

FIGURE 7. One-dimensional (planar averaged) streamwise energy spectrum at $Y = 0$ and $t = 92$ of the QUICK scalar (squares), the BQUICK scalar (crosses) and WENO scalar (circles).

$Z = 0.5$ for the BQUICK and WENO schemes. It is seen that the WENO does not show the small structures as the BQUICK scheme does. As a consequence this scheme is not able to capture small packets of low mixture fraction surrounded by high mixture fraction and vice versa. Consistent resolution of these situations will have a significant impact in increasing the predictive capability of LES.

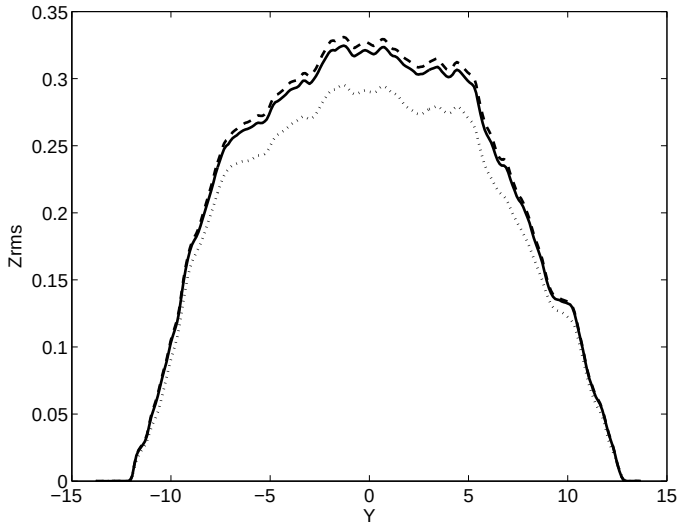

FIGURE 8. Plane averaged cross-stream profiles of mixture fraction obtained in the mixing layer at $Y = 0$ and $t = 92$. Dashed lines show QUICK profile, solid lines show BQUICK profile and, dotted lines show WENO profile.

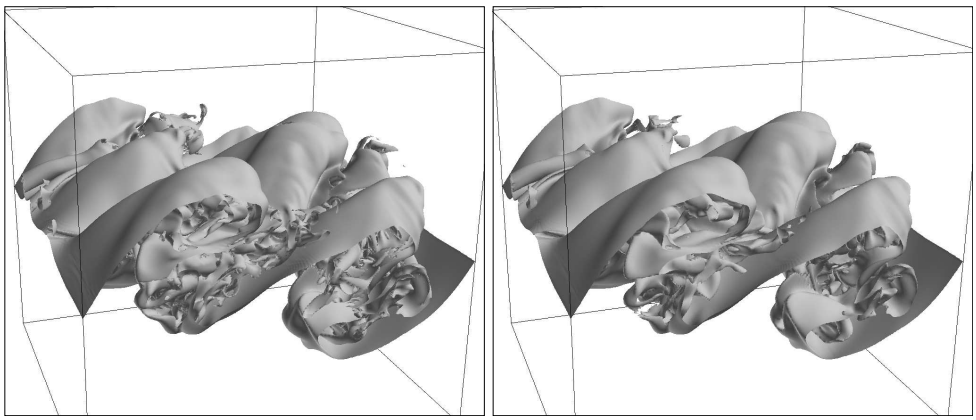

FIGURE 9. Iso-surface $Z = 0.5$ at $t = 46$ for the BQUICK scalar field (left) and the WENO scalar field (right).

5. Conclusion

In conclusion, these tests have clearly shown that the flux-corrected third-order scheme, BQUICK, is clearly superior to TVB based formulations or the original QUICK scheme without scalar bounds. This new scheme will be especially useful in combustion simulations with lean fuel mixture. The low stoichiometric mixture fraction associated with such fuel mixtures leads to very strong density gradients in the mixture-fraction space close to mixture-fraction value of 0. The QUICK scheme leads to extended excursions below 0 that can cause large and unphysical temporal change of density. This feeds itself into the continuity equation thereby leading to algorithmic instability. The BQUICK scheme has been successfully implemented in constant and variable density flows for both structured and unstructured grid based LES solvers. Preliminary calculations follow the

same trend as the simulations shown here. Results from this work will be communicated in the near future.

Acknowledgements

The authors would like to thank Frank Ham and Heinz Pitsch for fruitful discussions concerning WENO schemes.

REFERENCES

Ham, F., Apte, S., Iaccarino, G., Wu, X., Herrmann, M., Constantinescu, G., Mahesh, K. & Moin, P. 2003 Unstructured LES of reacting multiphase flows in realistic gas turbine combustors. In *Annual Research Briefs-2003*, pp. 139–160. Stanford, CA: Center for Turbulence Research.

Jiang, G.-S. & Peng, D. 2000 Weighted ENO schemes for Hamilton-Jacobi equations. *SIAM J. Sci. Comput.* **21** (6), 2126–2143.

Jiang, G. S. & Shu, C. W. 1996 Efficient implementation of weighted ENO schemes. *J. Comput. Phys.* **126**, 202–228.

Leonard, B. P. 1979 A stable and accurate convective modelling procedure basedon quadratic upstream interpolation. *Comput. Methods Appl. Mech. Engrg.* **19**, 59–98.

di Mare, F., Jones, W. P. & Menzies, K. R. 2004 Large eddy simulation of a model gas turbine combustor. *Comb. Flame* **137** (3), 278–294.

Morinishi, Y., Lund, T. S., Vasilyev, O. V. & Moin, P. 1998 Fully conservative higher order finite difference schemes for incompressible flow. *J. Comput. Phys* **143** (1), 90–124.

Pierce, C. D. 2001 Progress-variable approach for large-eddy simulation of turbulence combustion. PhD thesis, Stanford University.

Pope, S. B. 2000 *Turbulent Flows*. Cambridge University Press.

Vreman, B., Geurts, B., Kuerten, H. 1995 A priori tests of large eddy simulation of the compressible plane mixing layer. *J. Eng. Math* **29** (4), 299–327.

Zalesak, S. T. 1979 Fully multidimensional flux-corrected transport algorithms for fluids. *J. Comput. Phys.* **31**, 335–362.